Sequence of events from the onset to the demise of the Last Interglacial: evaluating strengths and limitations of chronologies used in climatic archives

A. Govin, E. Capron, P. C. Tzedakis, S. Verheyden, B. Ghaleb, C. Hillaire-Marcel, G. St-Onge, J. S. Stoner, F. Bassinot, L. Bazin, T. Blunier, N. Combourieu-Nebout, A. El Ouahabi, D. Genty, R. Gersonde, P. Jimenez-Amat, A. Landais, B. Martrat, V. Masson-Delmotte, F. Parrenin, M.-S. Seidenkrantz, D. Veres, C. Waelbroeck, R. Zahn

Supplementary material:

It contains 8 supplementary tables and 1 supplementary figure.

1 Table S 1: Decimal coordinates and references of sites included in Figure 2.

Site	Latitude	Longitude	References*
Ice cores			
NEEM	77.49	-51.20	NEEM community members (2013)
NorthGRIP	75.10	-42.32	NorthGRIP project members (2004)
TALDICE	-72.82	159.60	Masson-Delmotte et al., (2011); Buiron et al., (2011)
EDML	-75.00	0.00	Stenni et al., (2010); Masson-Delmotte et al., (2011)
EDC	-75.10	123.35	Jouzel et al., (2007)
Mt Moulton	-74.04	-134.70	Dunbar et al., (2008)
Dome F	-77.32	39.70	Kawamura et al., (2007)
Vostok	-78.47	106.87	Petit et al., (1999)
Corals			
Bahamas	24.05	-74.05	Thompson et al., (2011)
Sal Island	16.70	-22.90	Zazo et al., (2010)
Speleothems			
Entrische Kirche Cave	47.22	16.08	Meyer et al., (2008)
La Chaise Cave	46.67	0.50	Couchoud et al., (2009)
Maxange Cave	44.83	0.91	D. Genty & K. Wainer, unpublished
NALPS	47.40	9.70	Boch et al., (2011)
Tana che Urla Cave	44.02	10.35	Regattieri et al., (2014)
Corchia Cave	43.98	10.22	Drysdale et al., (2005; 2007; 2009)
Cobre Cave	42.98	-4.37	Osete et al., (2012); Rossi et al (2014)
Soreq Cave	31.75	35.03	Bar-Matthews et al., (2003)
Sanbao Cave	31.60	110.44	Wang et al., (2008); Cheng et al., (2009)
Daeya Cave	37.17	128.05	Jo et al., (2011)
Dongge Cave	26.27	108.25	Kelly et al., (2006); Yuan et al., (2004)

Remouchamps Cave	50.48	5.71	Juvigné and Gewelt (1988)
Bohon Cave	50.35	5.46	Gewelt and Juvigné (1986)
Santana Cave	-24.85	-49.20	Cruz et al., (2006a; 2006b)
Marine sediment cores			
ODP 980	55.80	-14.11	Oppo et al., (2006)
MD95-2042	37.84	-10.70	Shackleton et al., (2000; 2002; 2003)
ODP 1063	34.15	-58.03	Channel et al., (2012)
MD02-2488	-46.49	88.02	Govin et al., (2012)
Pollen sequence			
Ioannina	39.67	20.88	Tzedakis et al., (2003)
Lake sediment cores			
Lac du Bouchet	44.90	3.79	Thouveny et al., (1990)
Lago Grande di Monticchio	40.95	15.58	Brauer et al., (2007)

* The list of references associated to each site is not exhaustive and refer to the articles cited in the manuscript.

Table S 2: Decay constants of U-series isotopes used in radiometric age determinations with their uncertainties. These uncertainties correspond for LIG marine corals to potential age differences of up to about ± 0.8 or ± 1.3 ka (within a 95 % confidence interval) for the U-series time scale vs. absolute time, depending on the statistical approach used to assess them.

Isotope	Decay constant (y^{-1})	Reference
^{238}U	$1.55125\ E^{-10}\pm1.66462E^{-13}$	Jaffey et al., (1971)
^{234}U	$2.82629\ E^{-6}\pm5.63555E^{-9}$	Cheng et al., (2000)
^{230}Th	$9.15771E^{-6}\pm2.77833E^{-8}$	Cheng et al., (2000)
^{235}U	$9.8485E^{-10}\pm1.34151E^{-12}$	Jaffey et al., (1971)
^{231}Pa	$2.11583E^{-5}\pm1.41141E^{-7}$	Robert et al., (1969)

Table S 3: Orbital ice and gas age markers used to constrain the AICC2012 chronology over the time interval 140-100 ka (Bazin et al., 2013; Veres et al., 2013).

	Ice core	Depth (m)	Age (ka)	1σ (ka)	Markers	References
Ice age markers	Vostok	1675	121.8	4	O_2/N_2	Suwa & Bender (2008)
	Vostok	1853.7	132.3	4	O_2/N_2	Suwa & Bender (2008)
	Vostok	2012.6	143.9	4	O_2/N_2	Suwa & Bender (2008)
	EDC	1377.7	101	4	Air content	Raynaud et al., (2007)
	EDC	1790.3	143	6.5	Air content	Raynaud et al., (2007)
Gas age markers	Vostok	1602.4	110.6	6	$\delta^{18}O_{atm}$	Suwa & Bender (2008)
	Vostok	1764.6	121.9	6	$\delta^{18}O_{atm}$	Suwa & Bender (2008)
	Vostok	1941.6	133.5	6	$\delta^{18}O_{atm}$	Suwa & Bender (2008)
	Vostok	2057.4	145.4	6	$\delta^{18}O_{atm}$	Suwa & Bender (2008)

Table S 4: Ice and gas stratigraphic links, and associated 1σ uncertainties, used to constrain the AICC2012 chronology over the time interval 140-100 ka (Bazin et al., 2013; Veres et al., 2013).

GAS STRATIGRAPHIC LINKS							
EDML-EDC	EDML depth (m)	EDML resulting age (ka)	EDC depth (m)	EDC resulting AICC2012 age (ka)	Age uncertainty (ka)	Gas parameter	References
	2190.0	101.0	1427.3	101.3	0.8	CH_4	Schilt et al., (2010)
	2209.5	103.1	1445.2	103.2	1	CH_4	Bazin et al., (2013)
	2223.9	105.2	1463.0	105.2	3	$\delta^{18}O_{atm}$	Bazin et al., (2013)
	2230.4	106.2	1472.8	106.1	1	CH_4	Bazin et al., (2013)
	2230.5	106.3	1473.2	106.1	0.8	CH_4	Schilt et al., (2010)
	2233.8	106.8	1476.8	106.3	1.2	CH_4	Bazin et al., (2013)
	2236.5	107.3	1485.0	107.3	0.8	CH_4	Schilt et al., (2010)
	2259.9	110.9	1509.8	110.5	3	CH_4	Bazin et al., (2013)
	2262.7	111.2	1512.5	110.9	0.8	CH_4	Schilt et al., (2010)
	2300.0	116.6	1567.5	116.7	0.8	CH_4	Schilt et al., (2010)
	2309.9	118.0	1584.0	118.2	3	$\delta^{18}O_{atm}$	Bazin et al., (2013)
	2342.4	123.3	1650.2	123.5	3	$\delta^{18}O_{atm}$	Bazin et al., (2013)
	2366.9	128.4	1705.5	127.7	3	$\delta^{18}O_{atm}$	Bazin et al., (2013)
	2368.3	128.6	1718.8	128.5	0.8	CH_4	Schilt et al., (2010)
	2369.3	128.7	1721.5	128.7	1.2	CH_4	Bazin et al., (2013)
	2380.9	131.2	1746.3	130.4	2	$\delta^{18}O_{atm}$	Bazin et al., (2013)
	2382.3	131.4	1757.3	131.4	0.8	CH_4	Schilt et al., (2010)
EDC- Vostok	EDC depth (m)	EDC resulting age (ka)	Vostok depth (m)	Vostok resulting AICC2012 age (ka)	Age uncertainty (ka)	Gas parameter	References
	1423.0	101.0	1464.1	100.9	1.3	CH_4	Loulergue (2007)
	1462.4	105.2	1522.9	105.2	1.5	CH_4	Loulergue (2007)
	1463.0	105.2	1529.3	105.3	1.0	$\delta^{18}O_{atm}$	Bazin et al., (2013)
	1472.7	106.1	1537.0	106.0	1.0	CH_4	Bazin et al., (2013)
	1476.8	106.3	1542.1	106.4	1.0	CH_4	Bazin et al., (2013)
	1477.8	106.5	1536.1	106.0	1.5	CH_4	Loulergue (2007)
	1509.8	110.5	1592.0	110.7	1.2	$\delta^{18}O_{atm}$	Bazin et al., (2013)
	1541.5	114.2	1626.2	114.3	1.2	CH_4	Loulergue (2007)
	1584.0	118.2	1685.0	118.2	1.2	$\delta^{18}O_{atm}$	Bazin et al., (2013)
	1589.6	118.7	1760.9	122.6	3.0	CH_4	Loulergue (2007)
	1650.2	123.5	1784.3	123.9	1.0	$\delta^{18}O_{atm}$	Bazin et al., (2013)

	1694.3	126.9	1842.4	127.1	1.6	CH_4	Loulergue (2007)
	1705.5	127.7	1863.0	128.0	1.5	$\delta^{18}O_{atm}$	Bazin et al., (2013)
	1718.3	128.5	1868.4	128.3	1.2	CH_4	Loulergue (2007)
	1721.5	128.7	1881.1	129.2	1.0	CH_4	Bazin et al., (2013)
	1726.3	129.0	1887.3	129.3	1.6	CH_4	Loulergue (2007)
NGRIP-EDML	NGRIP depth (m)	NGRIP resulting age (ka)	EDML depth (m)	EDML resulting AICC2012 age (ka)	Age uncertainty (ka)	Gas parameter	References
	2897.4	101.9	2198.0	101.9	0.7	CH_4	Capron et al., (2010)
	2903.4	102.5	2204.5	102.5	0.7	CH_4	Capron et al., (2010)
	2911.7	103.3	2209.9	103.2	0.7	CH_4	Capron et al., (2010)
	2932.6	105.0	2224.9	105.5	1.0	$\delta^{18}O_{atm}$	Capron et al., (2010)
	2945.2	106.0	2230.4	106.2	0.7	CH_4	Capron et al., (2010)
	2948.5	106.4	2233.8	106.8	0.7	CH_4	Capron et al., (2010)
	2958.5	107.8	2239.0	107.7	0.7	CH_4	Capron et al., (2010)
NGRIP-Vostok	NGRIP depth (m)	NGRIP resulting age (ka)	Vostok depth (m)	Vostok resulting AICC2012 age (ka)	Age uncertainty (ka)	Gas parameter	References
	2897.4	101.9	1480.8	101.7	1.2	$\delta^{18}O_{atm}$	Landais et al., (2006)
	2944.7	105.9	1534.8	105.9	1	CH_4	Landais et al., (2006)
	2946.4	106.2	1538.0	106.1	1	$\delta^{18}O_{atm}$	Landais et al., (2006)
	3038.0	116.1	1643.2	115.6	1.2	$\delta^{18}O_{atm}$	Landais et al., (2006)
	3049.8	117.2	1678.4	117.9	1.2	$\delta^{18}O_{atm}$	Landais et al., (2006)
TALDICE-EDC	TALDICE depth (m)	TALDICE resulting age (ka)	EDC depth (m)	EDC resulting AICC2012 age (ka)	Age uncertainty (ka)	Gas parameter	References
	1367.1	101.4	1427.3	101.3	0.8	CH_4	Schüpbach et al., (2011)
	1368.4	102.0	1432.8	101.8	0.8	CH_4	Schüpbach et al., (2011)
	1374.75	106.1	1471.3	106.0	0.8	CH_4	Schüpbach et al., (2011)
	1380	110.6	1515.4	111.2	1	CH_4	Buiron et al., (2011)
	1385	114.8	1544.8	114.5	1.5	CH_4	Buiron et al., (2011)
	1394	120.4	1622.0	121.2	2	CH_4	Buiron et al., (2011)
	1410	128.4	1717.3	128.4	1	CH_4	Buiron et al., (2011)
TALDICE-EDML	TALDICE depth (m)	TALDICE resulting age (ka)	EDML depth (m)	EDML resulting AICC2012 age (ka)	Age uncertainty (ka)	Gas parameter	References
	1367.1	101.4	2196	101.6	0.5	CH_4	Schüpbach et al., (2011)
	1368.4	102.0	2199.32	102.0	0.5	CH_4	Schüpbach et al., (2011)

	1374.75	106.1	2228.99	106.0	0.5	CH_4	Schüpbach et al., (2011)
TALDICE-Vostok	TALDICE depth (m)	TALDICE resulting age (ka)	Vostok depth (m)	Vostok resulting AICC2012 age (ka)	Age uncertainty (ka)	Gas parameter	References
	1374.0	105.5	1535.0	105.9	1.5	$\delta^{18}O_{atm}$	Bazin et al., (2013)
	1390.4	118.3	1672.2	117.5	2.0	$\delta^{18}O_{atm}$	Bazin et al., (2013)
	1406.3	127.0	1853.2	127.6	2.0	$\delta^{18}O_{atm}$	Bazin et al., (2013)
ICE STRATIGRAPHIC LINKS							
EDML-EDC	EDML depth (m)	EDML resulting age (ka)	EDC depth (m)	EDC resulting AICC2012 age (ka)	Age uncertainty (ka)	Synchronisation parameter	References
	2211.32	104.5	1426.86	104.4	0.1	volcanic	Ruth et al., (2007) Severi et al., (2007)
	2213.01	104.7	1429.11	104.6	0.02	volcanic	Ruth et al., (2007) Severi et al., (2007)
	2215.23	104.9	1432.47	104.9	0.1	volcanic	Ruth et al., (2007) Severi et al., (2007)
	2273.06	114.0	1510.78	113.9	0.02	volcanic	Ruth et al., (2007) Severi et al., (2007)
	2294.09	116.7	1538.61	116.6	0.1	volcanic	Ruth et al., (2007) Severi et al., (2007)
EDC-Vostok	EDC depth (m)	EDC resulting age (ka)	Vostok depth (m)	Vostok resulting AICC2012 age (ka)	Age uncertainty (ka)	Synchronisation parameter	References
	1429.1	104.6	1465.0	104.5	0.3	volcanic	Parrenin et al., (2012)
	1439.9	105.6	1478.5	105.6	0.2	volcanic	Parrenin et al., (2012)
	1443.4	105.9	1483.1	105.9	0.2	volcanic	Parrenin et al., (2012)
	1447.7	106.3	1488.8	106.3	0.2	volcanic	Parrenin et al., (2012)
	1448.4	106.4	1489.7	106.4	0.2	volcanic	Parrenin et al., (2012)
	1451.0	106.7	1493.3	106.7	0.2	volcanic	Parrenin et al., (2012)
	1452.4	106.8	1495.2	106.8	0.2	volcanic	Parrenin et al., (2012)
	1454.7	107.1	1498.5	107.1	0.2	volcanic	Parrenin et al., (2012)
	1456.0	107.2	1500.3	107.2	0.2	volcanic	Parrenin et al., (2012)
	1456.6	107.3	1501.3	107.3	0.2	volcanic	Parrenin et al., (2012)
	1470.5	109.0	1521.8	109.0	0.3	volcanic	Parrenin et al., (2012)
	1481.0	110.2	1537.4	110.2	0.2	volcanic	Parrenin et al., (2012)
	1482.8	110.5	1540.2	110.5	0.2	volcanic	Parrenin et al., (2012)
	1489.2	111.3	1550.4	111.3	0.2	volcanic	Parrenin et al., (2012)

	1494.9	112.0	1559.2	112.0	0.2	volcanic	Parrenin et al., (2012)
	1502.6	113.0	1571.2	112.9	0.2	volcanic	Parrenin et al., (2012)
	1506.3	113.4	1576.7	113.4	0.2	volcanic	Parrenin et al., (2012)
	1510.1	113.8	1582.1	113.8	0.2	volcanic	Parrenin et al., (2012)
	1511.5	114.0	1584.0	114.0	0.2	volcanic	Parrenin et al., (2012)
	1538.6	116.6	1618.2	116.6	0.2	volcanic	Parrenin et al., (2012)
	1541.1	116.8	1621.2	116.8	0.2	volcanic	Parrenin et al., (2012)
	1554.6	117.9	1637.7	117.9	0.2	volcanic	Parrenin et al., (2012)
	1563.0	118.6	1648.6	118.6	0.2	volcanic	Parrenin et al., (2012)
	1572.7	119.4	1662.1	119.4	0.2	volcanic	Parrenin et al., (2012)
	1580.3	120.0	1673.0	120.0	0.2	volcanic	Parrenin et al., (2012)
	1580.8	120.1	1673.7	120.1	0.2	volcanic	Parrenin et al., (2012)
	1581.1	120.1	1674.2	120.1	0.2	volcanic	Parrenin et al., (2012)
	1587.2	120.6	1682.9	120.6	0.2	volcanic	Parrenin et al., (2012)
	1598.9	121.5	1699.7	121.5	0.2	volcanic	Parrenin et al., (2012)
	1604.1	121.9	1707.3	121.9	0.2	volcanic	Parrenin et al., (2012)
	1607.2	122.1	1711.5	122.1	0.2	volcanic	Parrenin et al., (2012)
	1610.1	122.4	1715.6	122.3	0.2	volcanic	Parrenin et al., (2012)
	1631.2	123.9	1743.6	123.9	0.2	volcanic	Parrenin et al., (2012)
	1676.0	127.4	1801.7	127.4	0.2	volcanic	Parrenin et al., (2012)
	1678.9	127.6	1805.4	127.6	0.2	volcanic	Parrenin et al., (2012)
	1684.0	127.9	1812.0	127.9	0.2	volcanic	Parrenin et al., (2012)
	1690.9	128.4	1820.8	128.4	0.2	volcanic	Parrenin et al., (2012)
	1696.7	128.7	1828.3	128.7	0.1	volcanic	Parrenin et al., (2012)
	1704.3	129.3	1838.3	129.2	0.1	volcanic	Parrenin et al., (2012)
	1708.9	129.6	1844.6	129.6	0.2	volcanic	Parrenin et al., (2012)
	1711.1	129.7	1847.7	129.7	0.1	volcanic	Parrenin et al., (2012)
	1716.9	130.1	1855.5	130.2	0.1	volcanic	Parrenin et al., (2012)
	1726.9	130.9	1869.7	130.9	0.2	volcanic	Parrenin et al., (2012)
	1731.8	131.3	1876.6	131.3	0.2	volcanic	Parrenin et al., (2012)
	1734.7	131.6	1880.8	131.6	0.2	volcanic	Parrenin et al., (2012)
	1745.9	132.8	1896.9	132.8	0.2	volcanic	Parrenin et al., (2012)
	1748.1	133.0	1899.9	133.0	0.2	volcanic	Parrenin et al., (2012)
	1767.4	135.5	1926.7	135.5	0.3	volcanic	Parrenin et al., (2012)
	1769.0	135.8	1929.0	135.7	0.3	volcanic	Parrenin et al., (2012)
	1771.5	136.2	1932.8	136.2	0.4	volcanic	Parrenin et al., (2012)
	1772.9	136.4	1934.9	136.4	0.4	volcanic	Parrenin et al., (2012)
	1781.6	138.0	1948.7	138.0	0.4	volcanic	Parrenin et al., (2012)
	1782.9	138.3	1951.0	138.3	0.3	volcanic	Parrenin et al., (2012)

	1789.2 1791.3	139.6 140.1	1962.7 1966.4	139.6 140.0	0.4 0.4	volcanic volcanic	Parrenin et al., (2012) Parrenin et al., (2012)
ΔDEPTH CONSTRAINTS							
NGRIP	NGRIP depth (m)	AICC2012 age (ka)					
	2890.2 2895.8 2936.5	101.7 102.2 105.7					Landais et al., (2006) Capron et al., (2010) Landais et al., (2006) Capron et al., (2010) Landais et al., (2006) Capron et al., (2010)

16

17 Table S 5: Summary of tephra layers identified in the North Atlantic and Nordic Seas during the period 140-100 ka (also see Davies et al., 2014).

Tephra horizons	Age estimate	Volcanic System	Geographic occurrence	References	Comment
"5e-base" (basaltic)	129.5 ka[2] (SPECMAP)		*Greenland Sea* HM71-19, HM79-31	Fronval et al., (1998)	Geochemically different from the "5e-Low/BAS-IV" tephra (Wastegård and Rasmussen, 2001)
5e-Low/BAS-IV (basaltic)	127 ka[2] (SPECMAP)	Iceland	*NE Atlantic* ENAM 33 *Norwegian Sea* MD95-2009	Wastegård & Rasmussen (2001) Wastegård & Rasmussen (2001)	Geochemically different from the "5e-base" tephra (Wastegård and Rasmussen, 2001)
5e-Eem/TAB-I (basaltic)	124.4 ka[3] (ss09sea)	Iceland (Katla)	*Norwegian Sea* MD99-2289	Brendryen et al., (2010)	
5e-Midt/RHY or 5e-Eem/Rhy-I (rhyolithic)	125-124 ka[2] (SPECMAP) 121.8 ka[3] (ss09sea)	Iceland (Grímsvötn)	*Norwegian Sea* MD95-2009 ODP 644, HM71-25 MD99-2289 *Greenland Sea* HM57-7, HM71-19, HM79-31 1243-1, 1244-2, 1245-1 1246-4, 907A, P57-7 *North Atlantic* MD99-2253	Wastegård & Rasmussen (2001) Fronval et al., (1998) Brendryen et al., (2010) Sjøholm et al., (1991) Fronval et al., (1998) Wallrabe-Adams & Lackschewitz (2003) Davies et al., (2014)	
"1798-1799 cm" (basaltic)	122 ka[4] (GICC05-modelext)	?	*North Atlantic* MD99-2253	Davies et al., (2014)	
5e-Top/BAS (basaltic)	-	Iceland	*NE Atlantic* ENAM 33	Wastegård & Rasmussen (2001)	
5e-Top/RHY (rhyolitic)	-	Iceland	*NE Atlantic* ENAM 33	Wastegård & Rasmussen (2001)	
5d-DO26s/TRACHY-I (basaltic)	116.7 ka[3] (ss09sea)	Jan Mayen	*Norwegian Sea* MD99-2289	Brendryen et al., (2010)	

"2490-2491 cm" (rhyolitic)	116.4 ka[5] (ss09sea, LR04)	Iceland (Öræfajökull)	*NE Atlantic* MD04-2822	Abbott et al., (2013)	Geochemically different from the 5e-Top/RHY and 5d-Low/RHY-I tephra (Abbott et al., 2013)
5d-Low/RHY-I/II/III (rhyolitic)	-	Iceland	*NE Atlantic* ENAM 33	Wastegård & Rasmussen (2001)	
5d-DO25i/RHY-I (rhyolithic)	112.5 ka[3] (ss09sea)		*Norwegian Sea* MD99-2289	Brendryen et al., (2010)	Same tephra as 5d-Low/RHY-II? (Brendryen et al., 2010)
5d-BAS-I/II/III [1] (basaltic)	111.5 ka[2] (SPECMAP)		*Norwegian Sea* HM71-25	Fronval et al., (1998)	
			Greenland Sea HM57-7, HM71-19	Fronval et al., (1998)	
			HM79-31	Fronval et al., (1998)	
5c-Midt/BAS-I or 5c-DO24s/BAS-I (basaltic)	104 ka[6] 106.5 ka[3] (ss09sea)	Iceland (Grímsvötn)	*Norwegian Sea* MD95-2009 MD99-2289	Wastegård & Rasmussen (2001) Brendryen et al., (2010)	
5c-DO23i/BAS-I (basaltic)	103.2 ka[3] (ss09sea)	Iceland (Grímsvötn)	*Norwegian Sea* MD99-2289	Brendryen et al., (2010)	

[1] Name of tephra layer after Haflidason et al., (2000).

[2] Age estimated from $\delta^{18}O$ alignment (Fronval et al., 1998) to the SPECMAP reference record (Martinson et al., 1987).

[3] Age estimated from the alignment of MD99-2289 Ca and Ti/K, to NGRIP ice $\delta^{18}O$ and magnetic susceptibility, respectively, using the Greenland ss09sea time scale (Brendryen et al., 2010).

[4] Age estimated from the alignment of core MD99-2253 (Davies et al., 2014) to NGRIP ice $\delta^{18}O$ on the GICC05modelext time scale (Wolff et al., 2010).

[5] Age estimated from the (1) alignment of *N. pachyderma sinistral* percentages from core MD04-2822 to NGRIP ice $\delta^{18}O$ on the Greenland ss09sea time scale and (2) benthic $\delta^{18}O$ alignment to the LR04 reference record (Abbott et al., 2013).

[6] Age estimated by Wastegård and Rasmussen (2001) (method not specified).

Table S 6: List of tie-points and associated age uncertainties (1σ) defined for five different alignment methods applied to the North Atlantic core MD95-2042 (Shackleton et al., 2002; 2003). The combined age uncertainty (last column of the table) is derived from the quadratic sum of individual uncertainties. Difficult to estimate, the age uncertainty related to the hypothesis underlying the alignment method is not included here (e.g. see footnote a).

Depth (cm)	Age (ka)	Alignment strategy	Matching error (ka)	Resolution of aligned record (ka)	Resolution of reference record (ka)	**Relative alignment uncertainty (ka)**	Dating error of reference chronology (ka)	**Combined age uncertainty (ka)**
A. Benthic foraminiferal $\delta^{18}O$ alignment to LR04								
2252.7	94.2		0.8	0.3	1	**1.3** [a]	4 [b]	**4.2** [a]
2404.2	108.0		0.8	0.4	1	**1.3** [a]	4 [b]	**4.2** [a]
2480.2	115.9		0.8	0.4	1	**1.3** [a]	4 [b]	**4.2** [a]
2580.9	127.4		0.8	0.3	1	**1.3** [a]	4 [b]	**4.2** [a]
2671.2	134.3		0.8	0.2	1	**1.3** [a]	4 [b]	**4.2** [a]
2773.1	140.7		0.8	0.5	1	**1.4** [a]	4 [b]	**4.2** [a]
B. Planktonic foraminiferal $\delta^{18}O$ alignment to ice core temperature records on AICC2012								
2338.5	101.8	alignment to NGRIP ice $\delta^{18}O$	0.5	0.2		**0.6**	1.5 [c]	**1.6**
2362.7	103.2	alignment to NGRIP ice $\delta^{18}O$	0.5	0.2		**0.5**	1.5 [c]	**1.6**
2394.9	105.8	alignment to NGRIP ice $\delta^{18}O$	0.5	0.3		**0.6**	1.5 [c]	**1.6**
2408.8	107.9	alignment to NGRIP ice $\delta^{18}O$	0.5	0.5	neglected	**0.7**	1.6 [c]	**1.7**
2439.1	112.6	alignment to NGRIP ice $\delta^{18}O$	0.5	0.4		**0.7**	1.7 [c]	**1.8**
2570.4	128.7	alignment to EDC CH_4	0.5	0.3		**0.6**	1.7 [c]	**1.8**
2650.9	133.9	alignment to EDC CH_4	1.5	0.2		**1.5**	2.2 [c]	**2.7**
2730.1	140.4	alignment to EDC CH_4	1.5	0.8		**1.7**	2.8 [c]	**3.3**
C. Planktonic foraminiferal $\delta^{18}O$ alignment to Corchia speleothem $\delta^{18}O$ record								
2338.4	102.6	alignment to Corchia CC28	0.5	0.3		**0.6**	0.4 [d]	**0.7**
2365.0	105.1	alignment to Corchia CC28	0.5	0.3		**0.6**	0.4 [d]	**0.7**
2395.9	109.0	alignment to Corchia CC28	0.5	0.4		**0.7**	0.6 [d]	**0.9**
2407.2	111.8	alignment to Corchia CC28	0.5	0.4		**0.7**	0.6 [d]	**0.9**
2439.2	114.9	alignment to Corchia CC28	0.5	0.3	neglected	**0.6**	0.9 [d]	**1.1**
2569.9	128.8	alignment to Corchia CC5	0.5	0.3		**0.6**	0.7 [d]	**0.9**
2610.1	131.5	alignment to Corchia CC5	1	0.3		**1.0**	1.2 [d]	**1.6**
2650.3	135.8	alignment to Corchia CC5	1	0.3		**1.0**	0.8 [d]	**1.3**
2729.9	139.2	alignment to Corchia CC5	1.5	0.5		**1.6**	0.8 [d]	**1.8**
D. Planktonic foraminiferal $\delta^{18}O$ alignment to GL_T_syn on ice core EDC3 time scale								
2338.1	101.4		0.5	0.1		**0.5**	1.5 [e]	**1.6**
2363.1	103.5		0.5	0.2	neglected	**0.6**	1.5 [e]	**1.6**
2394.8	106.5		0.5	0.3		**0.6**	1.5 [e]	**1.6**

2408.7	108.5		0.5	0.4		**0.6**	1.5 [e]	**1.6**
2443.5	111.5		0.5	0.4		**0.6**	1.5 [e]	**1.6**
2570.2	128.4		0.5	0.3		**0.6**	1.5 [e]	**1.6**
2650.2	134.4		1.5	0.2		**1.5**	3 [e]	**3.4**
2729.2	138.1		1.5	0.6		**1.6**	3 [e]	**3.4**
E. Planktonic foraminiferal $\delta^{18}O$ alignment to GL_T_syn on Chinese speleothem time scale								
2338.0	103.2		0.5	0.3		**0.6**	1.2 [f]	**1.4**
2363.1	106.3		0.5	0.3		**0.6**	1.6 [f]	**1.7**
2393.1	109.8		0.5	0.3		**0.6**	1.6 [f]	**1.7**
2408.7	111.3		0.5	0.3	neglected	**0.6**	1.6 [f]	**1.7**
2443.1	114.1		0.5	0.3		**0.6**	1.6 [f]	**1.7**
2570.2	129.1		0.5	0.3		**0.6**	1.4 [f]	**1.5**
2650.5	135.2		1.5	0.2		**1.5**	1.3 [f]	**2.0**
2730.4	138.3		1.5	0.5		**1.6**	1.5 [f]	**2.2**

[a] Caution: this age uncertainty does not include the age error related to the possibility of diachronous benthic $\delta^{18}O$ changes across water-masses, which may reach up to 4 ka during deglacations (e.g. Skinner and Shackleton, 2005; Waelbroeck et al., 2011). Including this additional error can lead to very large combined age uncertainties up to 6 ka during the penultimate deglaciation and the LIG.

[b] from Lisiecki & Raymo (2005).

[c] from Bazin et al., (2013); Veres et al., (2013).

[d] from Drysdale et al., (2007; 2009).

[e] from Parrenin et al., (2007).

[f] from Barker et al., (2011).

Table S 7: List of tie-points and associated age uncertainties (1σ) defined for two alignment methods in the Southern Ocean core MD02-2488 (Govin et al., 2009; 2012). The combined age uncertainty (last column of the table) is derived from the quadratic sum of individual uncertainties. Difficult to estimate, the age uncertainty related to the hypothesis underlying the alignment method is not included here (see footnote a).

Depth (cm)	Age (ka)	Alignment strategy	Matching error (ka)	Resolution of aligned record (ka)	Resolution of reference record (ka)	**Relative alignment uncertainty (ka)**	Dating error of reference chronology (ka)	**Combined age uncertainty (ka)**
A. Benthic foraminiferal $\delta^{18}O$ alignment to LR04								
2000.9	85.4		0.8	0.5	1.0	**1.4** [a]	4 [b]	**4.3** [a]
2324.0	106.2		0.8	0.5	1.0	**1.4** [a]	4 [b]	**4.3** [a]
2474.9	115.9		0.8	0.2	1.0	**1.3** [a]	4 [b]	**4.3** [a]
2539.6	126.6		0.8	0.2	1.0	**1.3** [a]	4 [b]	**4.3** [a]
2548.0	131.6		0.8	0.2	1.0	**1.3** [a]	4 [b]	**4.3** [a]
2595.6	134.5		0.8	0.3	1.0	**1.4** [a]	4 [b]	**4.3** [a]
B. Sea Surface Temperature alignment to ice core temperature records on AICC2012								
2250.9	102.6	alignment to EDC δD	0.5	0.5		**0.7**	1.7 [c]	**1.9**
2279.4	103.8	alignment to EDC δD	0.5	0.4		**0.7**	1.7 [c]	**1.9**
2330.2	106.7	alignment to EDC δD	0.5	0.2		**0.6**	1.8 [c]	**1.9**
2424.5	110.3	alignment to EDC δD	0.8	0.2	neglected	**0.9**	1.7 [c]	**2.0**
2503.0	117.4	alignment to EDC δD	1	0.2		**1.1**	1.7 [c]	**2.0**
2552.6	131.0	alignment to EDC δD	1	0.4		**1.1**	1.8 [c]	**2.2**
2658.5	135.9	alignment to EDC δD	0.8	0.4		**0.9**	2.5 [c]	**2.7**

[a] Caution: this age uncertainty does not include the age error related to the possibility of diachronous benthic $\delta^{18}O$ changes across water-masses, which may reach up to 4 ka during deglacations (e.g. Skinner and Shackleton, 2005; Waelbroeck et al., 2011). Including this additional error can lead to very large combined age uncertainties up to 6 ka during the penultimate deglaciation and the LIG.

[b] from Lisiecki & Raymo (2005).

[c] from Bazin et al., (2013); Veres et al., (2013).

Table S 8: List of remarkable events identified in major paleoclimatic records. We focused on (1) the onset of the deglacial period, (2) the onset of the LIG interval, (3) the demise of the LIG interval and (4) the establishment of glacial conditions (see Figure 1 for definitions of terms). Related (1σ) age uncertainties include (1) the "internal" error of the event (given by RAMPFIT), (2) the error related to the transfer of records on a specific time scale (for lake and marine sediments) and (3) the absolute dating error of the used time scale. The combined age uncertainty is derived from the quadratic sum of individual uncertainties. Events are defined using the RAMPFIT software (Mudelsee, 2000, code from 2013) or visually when impossible to fit reliable linear ramps through the record (see Method column). All ice core records are on the AICC2012 time scale (Bazin et al., 2013; Veres et al., 2013). The number in the 1st column refers to Figure 13.

#	Event age (ka)	Internal error of event (ka, 1σ)	Relative alignment error (ka, 1σ)	Error of reference age scale (ka, 1σ)	Combined age error (ka, 1σ)	Event	Method	Reference of record
1	139.7					Minimum in 65°N June 21 insolation	visual	Laskar et al., (2004)
2	130.8					Maximum in obliquity	visual	Laskar et al., (2004)
3	127.5					Maximum in 65°N June 21 insolation	visual	Laskar et al., (2004)
4	115.7					Minimum in 65°N June 21 insolation	visual	Laskar et al., (2004)
5	112.1					Minimum in obliquity	visual	Laskar et al., (2004)
6	104.8					Maximum in 65°N June 21 insolation	visual	Laskar et al., (2004)
7	137.8	0.5		2.6	2.7	EDC CO_2 starts increasing	rampfit	Schneider et al., (2013)
8	128.0	0.4		1.7	1.8	EDC CO_2 reaches LIG max values	rampfit	Schneider et al., (2013)
9	115.5	0.4		1.7	1.8	EDC CO_2 starts decreasing	rampfit	Schneider et al., (2013)
10	109.1	0.5		1.8	1.9	EDC CO_2 reaches glacial values	rampfit	Schneider et al., (2013)
11	137.1	0.6		2.6	2.7	EDC CH_4 starts increasing	rampfit	Loulergue et al., (2008)
12	128.5	0.1		1.8	1.9	EDC CH_4 reaches LIG max values	rampfit	Loulergue et al., (2008)
13	128.0	0.1		1.7	1.8	EDC CH_4 starts decreasing (step 1)	rampfit	Loulergue et al., (2008)
14	120.6	0.3		1.7	1.7	EDC CH_4 starts decreasing (step 2)	rampfit	Loulergue et al., (2008)
15	112.7	0.5		1.7	1.8	EDC CH_4 reaches min glacial values	rampfit	Loulergue et al., (2008)
16	135.6	0.1		2.5	2.5	EDC δD starts increasing	rampfit	Jouzel et al., (2007)
17	129.4	0.1		1.8	1.8	EDC δD reaches LIG max values	rampfit	Jouzel et al., (2007)
18	127.9	0.3		1.7	1.8	EDC δD starts decreasing (step 1)	rampfit	Jouzel et al., (2007)
19	120.3	0.3		1.7	1.7	EDC δD starts decreasing (step 2)	rampfit	Jouzel et al., (2007)
20	107.8	0.5		1.9	2.0	EDC δD reaches glacial values	rampfit	Jouzel et al., (2007)
21	127.3	0.1	1.5	1.8	2.4	NEEM temperature reaches LIG max values	rampfit	NEEM members (2013)
22	120.3	0.4	1.5	1.7	2.3	NEEM temperature starts decreasing	rampfit	NEEM members (2013)

23	107.7	0.2		1.6	1.6	NGRIP ice $\delta^{18}O$ reaches glacial values (= onset of GS-25)	visual	NGRIP members (2004)
24	133.4	0.1		0.9	0.9	Corchia $\delta^{18}O$ (CC5) starts decreasing	rampfit	Drysdale et al., (2009)
25	128.3	0.1		0.6	0.6	Corchia $\delta^{18}O$ (CC5) reaches LIG min values	rampfit	Drysdale et al., (2009)
26	126.9	0.0		0.5	0.6	Corchia $\delta^{18}O$ (CC5) starts increasing	rampfit	Drysdale et al., (2009)
27	130.3	0.1		0.35	0.4	Sanbao $\delta^{18}O$ (SB41) starts decreasing	rampfit	Wang et al., (2008)
28	130.0	0.1		0.1	0.1	Sanbao $\delta^{18}O$ (SB25) starts decreasing	rampfit	Cheng et al., (2009)
29	128.2	0.0		0.1	0.1	Sanbao $\delta^{18}O$ (SB25) reaches LIG min values	rampfit	Cheng et al., (2009)
30	126.7	0.1		0.8	0.8	Sanbao $\delta^{18}O$ (SB23) reaches LIG min values	rampfit	Wang et al., (2008)
31	125.3	0.1		0.40	0.5	Sanbao $\delta^{18}O$ (SB41) reaches LIG min values	rampfit	Wang et al., (2008)
32	122.0	0.1		0.7	0.8	Sanbao $\delta^{18}O$ (SB23) starts increasing	rampfit	Wang et al., (2008)
33	121.3	0.1		0.4	0.4	Sanbao $\delta^{18}O$ (SB41) starts increasing	rampfit	Wang et al., (2008)
34	117.4	0.2		0.6	0.7	Sanbao $\delta^{18}O$ (SB23) reaches glacial values	rampfit	Wang et al., (2008)
35	116.8	0.3		0.4	0.5	Sanbao $\delta^{18}O$ (SB41) reaches glacial values	rampfit	Wang et al., (2008)
36	129.0	0.2		1.6	1.6	Monticchio temperate tree pollen start increasing	rampfit	Brauer et al. (2007)
37	127.2	0.1		1.6	1.6	Monticchio temperate tree pollen reach LIG max values	visual? [b]	Brauer et al. (2007)
38	109.5	0.2		1.4	1.4	Monticchio temperate tree pollen start decreasing	visual? [b]	Brauer et al. (2007)
39	107.8	0.2		1.4	1.4	Monticchio temperate tree pollen reach glacial values	rampfit	Brauer et al. (2007)
40	132.3	0.4		2.3	2.3	Ioannina temperate tree pollen start increasing	rampfit	Tzedakis et al., (2003)
41	127.5	0.3		2.3	2.3	Ioannina Mediterranean Sclerophylls pollen reach LIG max values	visual	Tzedakis et al., (2003)
42	114.7	0.5		2.3	2.4	Ioannina temperate tree pollen start decreasing	visual	Tzedakis et al., (2003)
43	110.7	0.5		2.3	2.4	Ioannina temperate tree pollen reach glacial values	visual	Tzedakis et al., (2003)
44	130.1	0.6	1.1	1.8	2.2	North Atlantic (MD95-2042) benthic $\delta^{13}C$ starts increasing	rampfit	Shackleton et al., (2002; 2003)
45	125.9	0.5	0.6	1.8	2.0	North Atlantic (MD95-2042) benthic $\delta^{13}C$ reaches LIG max values	rampfit	Shackleton et al., (2002; 2003)
46	121.1	1.6	0.7	1.7	2.5	North Atlantic (MD95-2042) benthic $\delta^{13}C$ starts decreasing	rampfit	Shackleton et al., (2002; 2003)
47	106.0	1.5	0.6	1.75	2.5	North Atlantic (MD95-2042) benthic $\delta^{13}C$ reaches glacial values	rampfit	Shackleton et al., (2002; 2003)
48	131.9	0.0	1.1	2.0	2.3	Southern Ocean (MD02-2488) benthic $\delta^{13}C$ starts increasing	rampfit	Govin et al., (2009; 2012)
49	120.4	0.6	1.1	1.7	2.1	Southern Ocean (MD02-2488) benthic $\delta^{13}C$ reaches LIG max values	rampfit	Govin et al., (2009; 2012)

50	116.2	0.4	1.0	1.7	2.0	Southern Ocean (MD02-2488) benthic $\delta^{13}C$ starts decreasing	rampfit	Govin et al., (2009; 2012)
51	114.3	0.4	1.0	1.7	2.0	Southern Ocean (MD02-2488) benthic $\delta^{13}C$ reaches glacial values	rampfit	Govin et al., (2009; 2012)
52	129.0			1.0[a]	1.0[a]	Onset of the global sea level highstand	visual	Dutton et al., (2012)
53	116.0			0.8[a]	0.8[a]	End of the global sea level highstand	visual	Dutton et al., (2012)
54	135.3	0.2	2.0	2.4	3.2	Onset of North Atlantic (ODP 980) deglacial IRD peak	visual	Oppo et al., (2006)
55	128.8	0.2	0.5	1.7	1.9	End of North Atlantic (ODP 980) deglacial IRD peak	visual	Oppo et al., (2006)
56	107.3	0.1	1.0	1.6	1.9	Onset of C24 (GS-25) North Atlantic (ODP 980) IRD peak	visual	Oppo et al., (2006)

[a] Sea level dating uncertainties are taken from the far-field Western Australian sites and averaged over the periods 128-131 ka and 116-119 ka for the onset and the end of the LIG highstand, respectively (Dutton and Lambeck, 2012).

[b] Age given by Brauer et al. (2007).

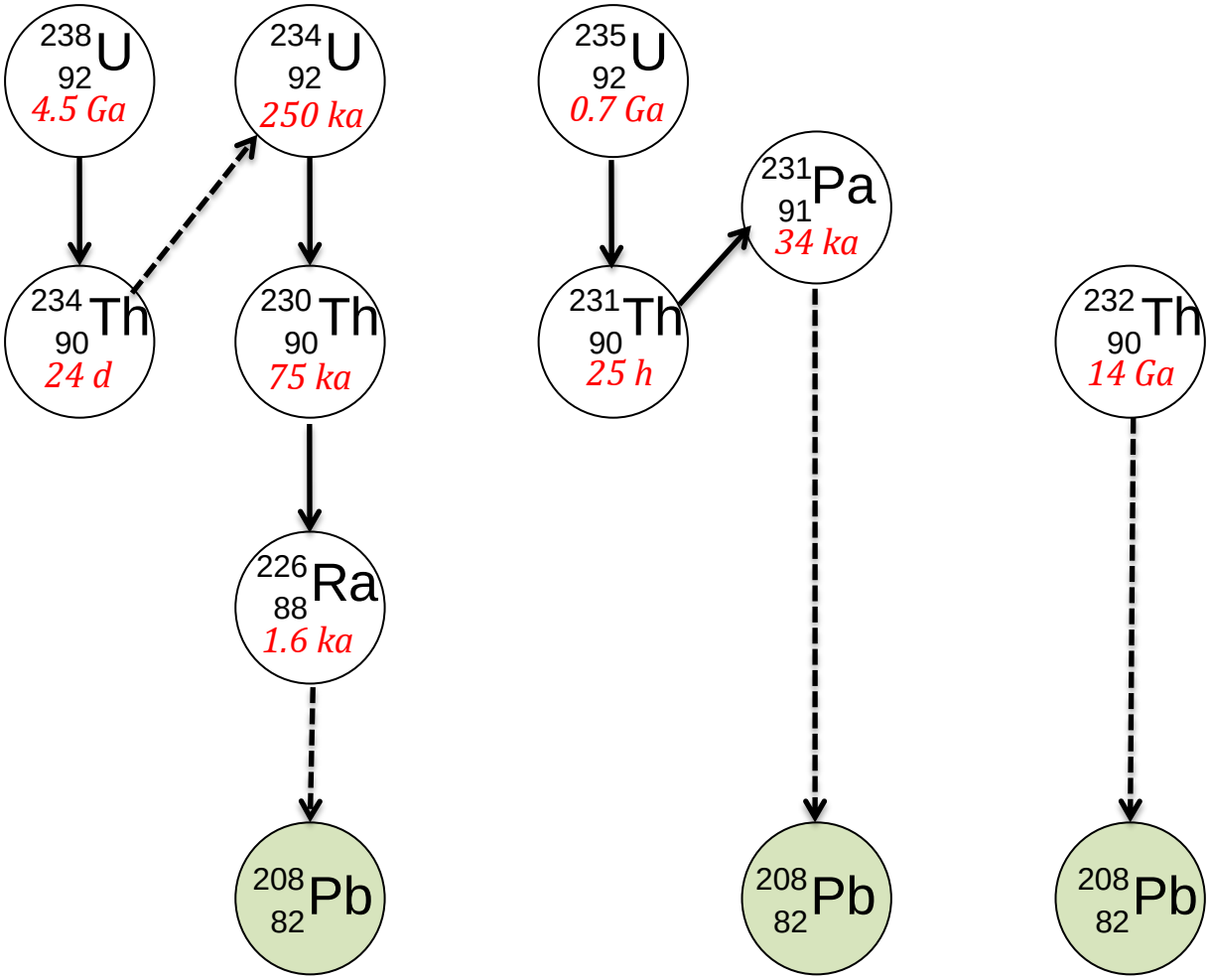
238 92 U
4.5 Ga
234 92 U
250 ka
235 92 U
0.7 Ga
231 91 Pa
34 ka
234 90 Th
24 d
230 90 Th
75 ka
231 90 Th
25 h
232 90 Th
14 Ga
226 88 Ra
1.6 ka
208 82 Pb
208 82 Pb
208 82 Pb

59

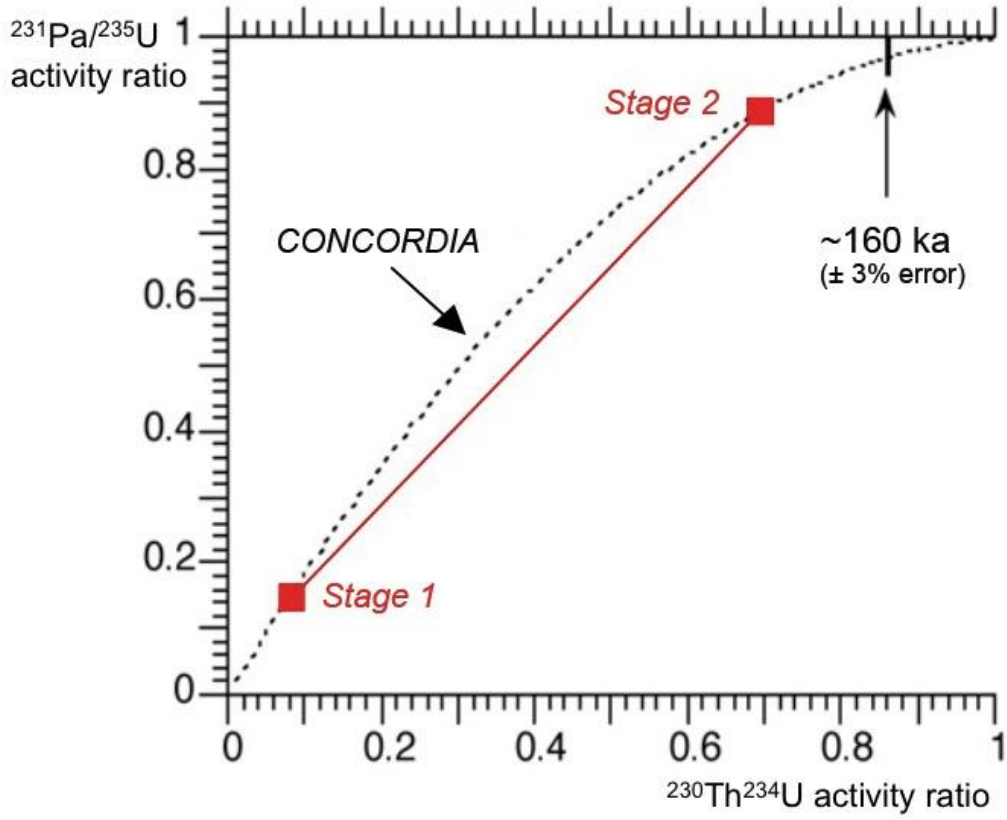
231Pa/235U activity ratio
1
0.8
0.6
0.4
0.2
0
Stage 2
CONCORDIA
~160 ka
(± 3% error)
Stage 1
0
0.2
0.4
0.6
0.8
1
230Th234U activity ratio

60

Figure S 1: *(Upper panel)* Simplified drawing of the ^{235}U, ^{238}U and ^{232}Th decay chains. Half-lives of radioactive isotopes (in gigayears (Ga), kiloyears (ka), and days (d) or hours (h)) are indicated in red italics. Green shading highlights stable Lead isotopes. U: Uranium; Th: Thorium; Pa: Protactinium; Ra: Radium; Pb: Lead. *(Lower panel)* The coupling of two radioactive chronometers ($^{231}Pa/^{235}U$ and $^{230}Th/^{234}U$) in a "concordia" diagram as illustrated here (adapted from Hillaire-Marcel 2009) may be used to evaluate the closure of the radioactive system. In a closed system, the sample will move along the "concordia curve" (dashed line) through time, whereas samples falling out of the "concordia curve" indicate the gain or loss of U-series isotopes within the radioactive system. The theoretical mixing line (in red) illustrates the situation when only two stages of U-uptake occurred (in this example: Stage 1 ~ LIG; Stage 2 ~ Holocene) (Hillaire-Marcel, 2009). However, uncertainties on ^{231}Pa measurements, on the initial $^{234}U/^{238}U$ composition of the coral uranium, and on decay constants, make $^{231}Pa/^{235}U$ vs. $^{230}Th/^{234}U$-^{238}U concordia ages rather imprecise, in particular for the LIG period. Complementary "pseudo-concordia" approaches may provide additional information on the closure of the radioactive system (see section 2.2 of the main text for details). 160 ka (i.e. around five times the half-life of ^{231}Pa) is the time range after which $^{231}Pa/^{235}U$ activity ratios get close to the secular equilibrium value (with a relative analytical precision of ± 3 %), i.e. after which such concordia diagrams cannot be used anymore.

References cited in the supplementary material

Abbott, P.M., Austin, W.E.N., Davies, S.M., Pearce, N.J.G., Hibbert, F.D., 2013. Cryptotephrochronology of the Eemian and the last interglacial–glacial transition in the North East Atlantic. Journal of Quaternary Science 28, 501-514, doi: 10.1002/jqs.2641.

Bar-Matthews, M., Ayalon, A., Gilmour, M., Matthews, A., Hawkesworth, C.J., 2003. Sea-land oxygen isotopic relationships from planktonic foraminifera and speleothems in the Eastern Mediterranean region and their implication for paleorainfall during interglacial intervals. Geochimica et Cosmochimica Acta 67, 3181-3199, doi: 10.1016/S0016-7037(02)01031-1.

Barker, S., Knorr, G., Edwards, R.L., Parrenin, F.d.r., Putnam, A.E., Skinner, L.C., Wolff, E., Ziegler, M., 2011. 800,000 Years of Abrupt Climate Variability. Science 334, 347-351, doi: 10.1126/science.1203580.

Bazin, L., Landais, A., Lemieux-Dudon, B., Toyé Mahamadou Kele, H., Veres, D., Parrenin, F., Martinerie, P., Ritz, C., Capron, E., Lipenkov, V., Loutre, M.F., Raynaud, D., Vinther, B., Svensson, A., Rasmussen, S.O., Severi, M., Blunier, T., Leuenberger, M., Fischer, H., Masson-Delmotte, V., Chappellaz, J., Wolff, E., 2013. An optimized multi-proxy, multi-site Antarctic ice and gas orbital chronology (AICC2012): 120-800 ka. Clim. Past 9, 1715-1731, doi: 10.5194/cp-9-1715-2013.

Boch, R., Cheng, H., Spötl, C., Edwards, R.L., Wang, X., Häuselmann, P., 2011. NALPS: a precisely dated European climate record 120-60 ka. Clim. Past 7, 1247-1259, doi: 10.5194/cp-7-1247-2011.

Brauer, A., Allen, J.R.M., Mingram, J., Dulski, P., Wulf, S., Huntley, B., 2007. Evidence for last interglacial chronology and environmental change from Southern Europe. Proceedings of the National Academy of Sciences 104, 450-455, doi: 10.1073/pnas.0603321104.

Brendryen, J., Haflidason, H., Sejrup, H.P., 2010. Norwegian Sea tephrostratigraphy of marine isotope stages 4 and 5: Prospects and problems for tephrochronology in the North Atlantic region. Quaternary Science Reviews 29, 847-864, doi: 10.1016/j.quascirev.2009.12.004.

Buiron, D., Chappellaz, J., Stenni, B., Frezzotti, M., Baumgartner, M., Capron, E., Landais, A., Lemieux-Dudon, B., Masson-Delmotte, V., Montagnat, M., Parrenin, F., Schilt, A., 2011. TALDICE-1 age scale of the Talos Dome deep ice core, East Antarctica. Clim. Past 7, 1-16, doi: 10.5194/cp-7-1-2011.

Capron, E., Landais, A., Lemieux-Dudon, B., Schilt, A., Masson-Delmotte, V., Buiron, D., Chappellaz, J., Dahl-Jensen, D., Johnsen, S., Leuenberger, M., Loulergue, L., Oerter, H., 2010. Synchronising EDML and NorthGRIP ice cores using δ18O of atmospheric oxygen (δ18Oatm) and CH4 measurements over MIS5 (80-123 kyr). Quaternary Science Reviews 29, 222-234, doi: 10.1016/j.quascirev.2009.07.014.

Channell, J.E.T., Hodell, D.A., Curtis, J.H., 2012. ODP Site 1063 (Bermuda Rise) revisited: Oxygen isotopes, excursions and paleointensity in the Brunhes Chron. Geochemistry, Geophysics, Geosystems 13, Q02001, doi: 10.1029/2011gc003897.

Cheng, H., Edwards, R.L., Broecker, W.S., Denton, G.H., Kong, X., Wang, Y., Zhang, R., Wang, X., 2009. Ice Age Terminations. Science 326, 248-252, doi: 10.1126/science.1177840.

Cheng, H., Edwards, R.L., Hoff, J., Gallup, C.D., Richards, D.A., Asmerom, Y., 2000. The half-lives of uranium-234 and thorium-230. Chemical Geology 169, 17-33, doi: 10.1016/S0009-2541(99)00157-6.

Couchoud, I., Genty, D., Hoffmann, D., Drysdale, R., Blamart, D., 2009. Millennial-scale climate variability during the Last Interglacial recorded in a speleothem from south-western France. Quaternary Science Reviews 28, 3263-3274, doi: 10.1016/j.quascirev.2009.08.014.

Cruz, F.W., Burns, S.J., Karmann, I., Sharp, W.D., Vuille, M., Ferrari, J.A., 2006a. A stalagmite record of changes in atmospheric circulation and soil processes in the Brazilian subtropics during the Late Pleistocene. Quaternary Science Reviews 25, 2749-2761, doi: 10.1016/j.quascirev.2006.02.019.

Cruz, J.F.W., Burns, S.J., Karmann, I., Sharp, W.D., Vuille, M., 2006b. Reconstruction of regional atmospheric circulation features during the late Pleistocene in subtropical Brazil from oxygen isotope composition of speleothems. Earth and Planetary Science Letters 248, 495-507, doi: 10.1016/j.epsl.2006.06.019.

Davies, S.M., Abbott, P.M., Meara, R.H., Pearce, N.J.G., Austin, W.E.N., Chapman, M.R., Svensson, A., Bigler, M., Rasmussen, T.L., Rasmussen, S.O., Farmer, E.J., 2014. A North Atlantic tephrostratigraphical framework for

130-60 ka b2k: new tephra discoveries, marine-based correlations, and future challenges. Quaternary Science Reviews 106, 101-121, doi: 10.1016/j.quascirev.2014.03.024.

Drysdale, R.N., Hellstrom, J.C., Zanchetta, G., Fallick, A.E., Sanchez Goni, M.F., Couchoud, I., McDonald, J., Maas, R., Lohmann, G., Isola, I., 2009. Evidence for Obliquity Forcing of Glacial Termination II. Science 325, 1527-1531, doi: 10.1126/science.1170371.

Drysdale, R.N., Zanchetta, G., Hellstrom, J.C., Fallick, A.E., McDonald, J., Cartwright, I., 2007. Stalagmite evidence for the precise timing of North Atlantic cold events during the early last glacial. Geology 35, 77-80, doi: 10.1130/g23161a.1.

Drysdale, R.N., Zanchetta, G., Hellstrom, J.C., Fallick, A.E., Zhao, J.-x., 2005. Stalagmite evidence for the onset of the Last Interglacial in southern Europe at 129 ± 1 ka. Geophys. Res. Lett. 32, doi: 10.1029/2005gl024658.

Dunbar, N.W., McIntosh, W.C., Esser, R.P., 2008. Physical setting and tephrochronology of the summit caldera ice record at Mount Moulton, West Antarctica. Geol. Soc. Am. Bull., 796–812, doi: 10.1130/B26140.1.

Dutton, A., Lambeck, K., 2012. Ice Volume and Sea Level During the Last Interglacial. Science 337, 216-219, doi: 10.1126/science.1205749.

Fronval, T., Jansen, E., Haflidason, H., Sejrup, H.P., 1998. Variability in surface and deep water conditions in the Nordic Seas during the last interglacial period. Quaternary Science Reviews 17, 963-985, doi: 10.1016/S0277-3791(98)00038-9.

Gewelt, M., Juvigné, E., 1986. Les 'Tephra de Remouchamps', un nouveau marqueur stratigraphique dans le Pleistocène supérieur daté par 230Th/ 234O dans des concrétions stalagmitiques. Annales de la Société géologique de Belgique 109, 489-497, doi:

Govin, A., Braconnot, P., Capron, E., Cortijo, E., Duplessy, J.C., Jansen, E., Labeyrie, L., Landais, A., Marti, O., Michel, E., Mosquet, E., Risebrobakken, B., Swingedouw, D., Waelbroeck, C., 2012. Persistent influence of ice sheet melting on high northern latitude climate during the early Last Interglacial. Clim. Past 8, 483-507, doi: 10.5194/cp-8-483-2012.

Govin, A., Michel, E., Labeyrie, L., Waelbroeck, C., Dewilde, F., Jansen, E., 2009. Evidence for northward expansion of Antarctic Bottom Water mass in the Southern Ocean during the last glacial inception. Paleoceanography 24, PA1202, doi: doi: 10.1029/2008PA001603.

Haflidason, H., Eiriksson, J., Kreveld, S.V., 2000. The tephrochronology of Iceland and the North Atlantic region during the Middle and Late Quaternary: a review. Journal of Quaternary Science 15, 3-22, doi: 10.1002/(sici)1099-1417(200001)15:1<3::aid-jqs530>3.0.co;2-w.

Hillaire-Marcel, C., 2009. The U-series dating of (biogenic) carbonates. IOP Conf. Series: Earth and Environmental Science.

Jaffey, A.H., Flynn, K.F., Glendenin, L.E., Bentley, W.C., Essling, A.M., 1971. Precision Measurement of Half-Lives and Specific Activities of U235 and U238. Physical Review C 4, 1889-1906, doi: 10.1103/PhysRevC.4.1889.

Jo, K.-n., Woo, K.S., Lim, H.S., Cheng, H., Edwards, R.L., Wang, Y., Jiang, X., Kim, R., Lee, J.I., Yoon, H.I., Yoo, K.-C., 2011. Holocene and Eemian climatic optima in the Korean Peninsula based on textural and carbon isotopic records from the stalagmite of the Daeya Cave, South Korea. Quaternary Science Reviews 30, 1218-1231, doi: 10.1016/j.quascirev.2011.02.012.

Jouzel, J., Masson-Delmotte, V., Cattani, O., Dreyfus, G., Falourd, S., Hoffmann, G., Minster, B., Nouet, J., Barnola, J.M., Chappellaz, J., Fischer, H., Gallet, J.C., Johnsen, S., Leuenberger, M., Loulergue, L., Luethi, D., Oerter, H., Parrenin, F., Raisbeck, G., Raynaud, D., Schilt, A., Schwander, J., Selmo, E., Souchez, R., Spahni, R., Stauffer, B., Steffensen, J.P., Stenni, B., Stocker, T.F., Tison, J.L., Werner, M., Wolff, E.W., 2007. Orbital and Millennial Antarctic Climate Variability over the Past 800,000 Years. Science 317, 793-796, doi: doi: 10.1126/science.1141038.

Juvigné, E., Gewelt, M., 1988. Téphra et dépôts des grottes. Intérêt stratigraphique réciproque, Annales de la Société géologique de Belgique, vol. 11, pp. 135-140.

Kawamura, K., Parrenin, F., Lisiecki, L., Uemura, R., Vimeux, F., Severinghaus, J., Hutterli, M.A., Nakazawa, T., Aoki, S., Jouzel, J., Raymo, M.E., Matsumoto, K., Nakata, H., Motoyama, H., Fujita, S., Goto-Azuma, K., Fujii,

Y., Watanabe, O., 2007. Northern Hemisphere forcing of climatic cycles in Antarctica over the past 360,000 years. Nature 448, 912-916, doi: 10.1038/nature06015.

Kelly, M.J., Edwards, R.L., Cheng, H., Yuan, D., Cai, Y., Zhang, M., Lin, Y., An, Z., 2006. High resolution characterization of the Asian Monsoon between 146,000 and 99,000 years B.P. from Dongge Cave, China and global correlation of events surrounding Termination II. Palaeogeography, Palaeoclimatology, Palaeoecology 236, 20-38, doi: 10.1016/j.palaeo.2005.11.042.

Landais, A., Masson-Delmotte, V., Jouzel, J., Raynaud, D., Johnsen, S., Huber, C., Leuenberger, M., Schwander, J., Minster, B., 2006. The glacial inception as recorded in the NorthGRIP Greenland ice core: timing, structure and associated abrupt temperature changes. Climate Dynamics 26, 273-284, doi: 10.1007/s00382-005-0063-y.

Laskar, J., Robutel, P., Joutel, F., Gastineau, M., Correia, A.C.M., Levrard, B., 2004. A long-term numerical solution for the insolation quantities of the Earth. Astronomy and Astrophysics 428, 261-285, doi: 10.1051/0004-6361:20041335.

Lisiecki, L.E., Raymo, M.E., 2005. A Pliocene-Pleistocene stack of 57 globally distributed benthic δ18O records. Paleoceanography 20, PA1003, doi: 10.1029/2004pa001071.

Loulergue, L., 2007. Contraintes chronologiques et biogéochimiques grâce au méthane dans la glace naturelle : une application aux forages du projet EPICA. Université Joseph Fourrier, Grenoble, France, p. 257

Loulergue, L., Schilt, A., Spahni, R., Masson-Delmotte, V., Blunier, T., Lemieux, B., Barnola, J.M., Raynaud, D., Stocker, T.F., Chappellaz, J., 2008. Orbital and millennial-scale features of atmospheric CH_4 over the past 800,000 years. Nature 453, 383-386, doi: 10.1038/nature06950.

Martinson, D.G., Pisias, N.G., Hays, J.D., Imbrie, J., Moore Jr, T.C., Shackleton, N.J., 1987. Age dating and the orbital theory of the ice ages: Development of a high-resolution 0 to 300,000-year chronostratigraphy. Quaternary Research 27, 1-29, doi: 10.1016/0033-5894(87)90046-9.

Masson-Delmotte, V., Buiron, D., Ekaykin, A., Frezzotti, M., Gallée, H., Jouzel, J., Krinner, G., Landais, A., Motoyama, H., Oerter, H., Pol, K., Pollard, D., Ritz, C., Schlosser, E., Sime, L.C., Sodemann, H., Stenni, B., Uemura, R., Vimeux, F., 2011. A comparison of the present and last interglacial periods in six Antarctic ice cores. Clim. Past 7, 397-423, doi: 10.5194/cp-7-397-2011.

Meyer, M.C., Spötl, C., Mangini, A., 2008. The demise of the Last Interglacial recorded in isotopically dated speleothems from the Alps. Quaternary Science Reviews 27, 476-496, doi: 10.1016/j.quascirev.2007.11.005.

Mudelsee, M., 2000. Ramp function regression: a tool for quantifying climate transitions. Computers & Geosciences 26, 293-307, doi: 10.1016/S0098-3004(99)00141-7.

NEEM community members, 2013. Eemian interglacial reconstructed from a Greenland folded ice core. Nature 493, 489-494, doi: 10.1038/nature11789.

North Greenland Ice Core Project members, 2004. High-resolution climate record of Northern Hemisphere climate extending into the last interglacial period. Nature 431, 147-151, doi: 10.1038/nature02805.

Oppo, D.W., McManus, J.F., Cullen, J., 2006. Evolution and demise of the last interglacial warmth in the subpolar North Atlantic. Quaternary Science Reviews 25, 3268-3277, doi: 10.1016/j.quascirev.2006.07.006.

Osete, M.-L., Martén-Chivelet, J., Rossi, C., Edwards, R.L., Egli, R., Muñoz-Garcéa, M.B., Wang, X., Pavón-Carrasco, F.J., Heller, F., 2012. The Blake geomagnetic excursion recorded in a radiometrically dated speleothem. Earth and Planetary Science Letters 353-354, 173-181, doi: 10.1016/j.epsl.2012.07.041.

Parrenin, F., Barnola, J.-M., Beer, J., Blunier, T., Castellano, E., Chappellaz, J., Dreyfus, G., Fischer, H., Fujita, S., Jouzel, J., Kawamura, K., Lemieux-Dudon, B., Loulergue, L., Masson-Delmotte, V., Narcisi, B., Petit, J.-R., Raisbeck, G., Raynaud, D., Ruth, U., Schwander, J., Severi, M., Spahni, R., Steffensen, J.P., Svensson, A., Udisti, R., Waelbroeck, C., Wolff, E., 2007. The EDC3 chronology for the EPICA Dome C ice core. Clim. Past 3, 485-497, doi: 10.5194/cp-3-485-2007.

Parrenin, F., Petit, J.-R., Masson-Delmotte, V., Wolff, E., Basile-Doelsch, I., Jouzel, J., Lipenkov, V., Rasmussen, S.O., Schwander, J., S., M., , Udisti, R., Veres, D., Vinther, B.M., 2012. Volcanic synchronisation between the EPICA Dome C and Vostok ice cores (Antarctica) 0-145 kyr BP. Climate of the Past 8, 1031-1045, doi: 10.5194/cp-8-1031-2012.

Petit, J.R., Jouzel, J., Raynaud, D., Barkov, N.I., Barnola, J.M., Basile, I., Bender, M.L., Chappellaz, J., Davis, M., Delaygue, G., Delmotte, M., Kotlyakov, V.M., Legrand, M., Lipenkov, V.Y., Lorius, C., Pépin, L., Ritz, C., Saltzman, E., Stievenard, M., 1999. Climate and atmospheric history of the past 420,000 years from the Vostok ice core, Antarctica. Nature 399, 429-436, doi: 10.1038/20859.

Raynaud, D., Lipenkov, V., Lemieux-Dudon, B., Duval, P., Loutre, M.-F., Lhomme, N., 2007. The local insolation signature of air content in Antarctic ice. A new step toward an absolute dating of ice records. Earth Planetary Science Letters 261, 337-349, doi: 10.1016/j.epsl.2007.06.025.

Regattieri, E., Zanchetta, G., Drysdale, R.N., Isola, I., Hellstrom, J.C., Roncioni, A., 2014. A continuous stable isotope record from the penultimate glacial maximum to the Last Interglacial (159–121 ka) from Tana Che Urla Cave (Apuan Alps, central Italy). Quaternary Research 82, 450-461, doi: 10.1016/j.yqres.2014.05.005.

Robert, F., Miranda, C.F., Muxart, R., 1969. Mesure de la période du protactinium-231 par microcalorimetrie. Radiochimica Acta 11, 104-108, doi: 10.1524/ract.1969.11.2.104.

Rossi, C., Mertz-Kraus, R., Osete, M.-L., 2014. Paleoclimate variability during the Blake geomagnetic excursion (MIS 5d) deduced from a speleothem record. Quaternary Science Reviews 102, 166-180, doi: 10.1016/j.quascirev.2014.08.007.

Ruth, U., Barnola, J.M., Beer, J., Bigler, M., Blunier, T., Castellano, E., Fischer, H., Fundel, F., Huybrechts, P., Kaufmann, P., Kipfstuhl, S., Lambrecht, A., Morganti, A., Oerter, H., Parrenin, F., Rybak, O., Severi, M., Udisti, R., Wilhelms, F., Wolff, E., 2007. "EDML1": a chronology for the EPICA deep ice core from Dronning Maud Land, Antarctica, over the last 150 000 years. Clim. Past 3, 475-484, doi: 10.5194/cp-3-475-2007.

Schilt, A., Baumgartner, M., Schwander, J., Buiron, D., Capron, E., Chappellaz, J., Loulergue, L., Schüpbach, S., Spahni, R., Fischer, H., Stocker, T.F., 2010. Atmospheric nitrous oxide during the last 140,000 years. Earth and Planetary Science Letters 300, 33-43, doi: doi: 10.1016/j.epsl.2010.09.027.

Schneider, R., Schmitt, J., Köhler, P., Joos, F., Fischer, H., 2013. A reconstruction of atmospheric carbon dioxide and its stable carbon isotopic composition from the penultimate glacial maximum to the last glacial inception. Clim. Past 9, 2507-2523, doi: 10.5194/cp-9-2507-2013.

Schüpbach, S., Federer, U., Bigler, M., Fischer, H., Stocker, T.F., 2011. A refined TALDICE-1a age scale from 55 to 112 ka before present for the Talos Dome ice core based on high-resolution methane measurements. Clim. Past 7, 1001-1009, doi: 10.5194/cp-7-1001-2011.

Severi, M., Becagli, S., Castellano, E., Morganti, A., Traversi, R., Udisti, R., Ruth, U., Fischer, H., Huybrechts, P., Wolff, E., Parrenin, F., Kaufmann, P., Lambert, F., Steffensen, J.P., 2007. Synchronisation of the EDML and EDC ice cores for the last 52 kyr by volcanic signature matching. Clim. Past 3, 367-374, doi: 10.5194/cp-3-367-2007.

Shackleton, N.J., Chapman, M.R., Sanchez-Goni, M.F., Pailler, D., Lancelot, Y., 2002. The classic Marine Isotope Substage 5e. Quaternary Research 58, 14-16, doi: 10.1006/qres.2001.2312.

Shackleton, N.J., Hall, M.A., Vincent, E., 2000. Phase relationships between millenial-scale events 64,000-24,000 years ago. Paleoceanography 15, 565-569, doi: 10.1029/2000PA000513.

Shackleton, N.J., Sanchez-Goni, M.F., Pailler, D., Lancelot, Y., 2003. Marine Isotope Substage 5e and the Eemian Interglacial. Global and Planetary Change 36, 151-155, doi: 10.1016/S0921-8181(02)00181-9.

Sjøholm, J., Sejrup, H.P., Furnes, H., 1991. Quaternary volcanic ash zones on the Iceland Plateau, southern Norwegian Sea. Journal of Quaternary Science 6, 159-173, doi: 10.1002/jqs.3390060205.

Skinner, L.C., Shackleton, N.J., 2005. An Atlantic lead over Pacific deep-water change across Termination I: implications for the application of the marine isotope stage stratigraphy. Quaternary Science Reviews 24, 571-580, doi: 10.1016/j.quascirev.2004.11.008.

Stenni, B., Masson-Delmotte, V., Selmo, E., Oerter, H., Meyer, H., Röthlisberger, R., Jouzel, J., Cattani, O., Falourd, S., Fischer, H., Hoffmann, G., Iacumin, P., Johnsen, S.J., Minster, B., Udisti, R., 2010. The deuterium excess records of EPICA Dome C and Dronning Maud Land ice cores (East Antarctica). Quaternary Science Reviews 29, 146-159, doi: doi: 10.1016/j.quascirev.2009.10.009.

Suwa, M., Bender, M.L., 2008. Chronology of the Vostok ice core constrained by O_2/N_2 ratios of occluded air, and its implication for the Vostok climate records. Quaternary Science Reviews 27, 1093-1106, doi: 10.1016/j.quascirev.2008.02.017.

Thompson, W.G., Allen Curran, H., Wilson, M.A., White, B., 2011. Sea-level oscillations during the last interglacial highstand recorded by Bahamas corals. Nature Geosci 4, 684-687, doi: 10.1038/ngeo1253.

Thouveny, N., Creer, K.M., Blunk, I., 1990. Extension of the Lac du Bouchet palaeomagnetic record over the last 120,000 years. Earth and Planetary Science Letters 97, 140-161, doi: 10.1016/0012-821X(90)90105-7.

Tzedakis, P.C., Frogley, M.R., Heaton, T.H.E., 2003. Last Interglacial conditions in southern Europe: evidence from Ioannina, northwest Greece. Global and Planetary Change 36, 157-170, doi: 10.1016/S0921-8181(02)00182-0.

Veres, D., Bazin, L., Landais, A., Toyé Mahamadou Kele, H., Lemieux-Dudon, B., Parrenin, F., Martinerie, P., Blayo, E., Blunier, T., Capron, E., Chappellaz, J., Rasmussen, S.O., Severi, M., Svensson, A., Vinther, B., Wolff, E.W., 2013. The Antarctic ice core chronology (AICC2012): an optimized multi-parameter and multi-site dating approach for the last 120 thousand years. Clim. Past 9, 1733-1748, doi: 10.5194/cp-9-1733-2013.

Waelbroeck, C., Skinner, L.C., Labeyrie, L., Duplessy, J.C., Michel, E., Vazquez Riveiros, N., Gherardi, J.M., Dewilde, F., 2011. The timing of deglacial circulation changes in the Atlantic. Paleoceanography 26, PA3213, doi: 10.1029/2010pa002007.

Wallrabe-Adams, H.-J., Lackschewitz, K.S., 2003. Chemical composition, distribution, and origin of silicic volcanic ash layers in the Greenland-Iceland-Norwegian Sea: explosive volcanism from 10 to 300 ka as recorded in deep-sea sediments. Marine geology 193, 273-293, doi: 10.1016/S0025-3227(02)00661-8.

Wang, Y., Cheng, H., Edwards, R.L., Kong, X., Shao, X., Chen, S., Wu, J., Jiang, X., Wang, X., An, Z., 2008. Millennial- and orbital-scale changes in the East Asian monsoon over the past 224,000 years. Nature 451, 1090-1093, doi: 10.1038/nature06692.

Wastegård, S., Rasmussen, T.L., 2001. New tephra horizons from Oxygen Isotope Stage 5 in the North Atlantic: correlation potential for terrestrial, marine and ice-core archives. Quaternary Science Reviews 20, 1587-1593, doi: 10.1016/S0277-3791(01)00055-5.

Wolff, E.W., Chappellaz, J., Blunier, T., Rasmussen, S.O., Svensson, A., 2010. Millennial-scale variability during the last glacial: The ice core record. Quaternary Science Reviews 29, 2828-2838, doi: 10.1016/j.quascirev.2009.10.013.

Yuan, D., Cheng, H., Edwards, R.L., Dykoski, C.A., Kelly, M.J., Zhang, M., Qing, J., Lin, Y., Wang, Y., Wu, J., Dorale, J.A., An, Z., Cai, Y., 2004. Timing, Duration, and Transitions of the Last Interglacial Asian Monsoon. Science 304, 575-578, doi: 10.1126/science.1091220.

Zazo, C., Goy, J.L., Hillaire-Marcel, C., Dabrio, C.J., Gonzalez-Delgado, J.A., Cabero, A., Bardaji, T., Ghaleb, B., Soler, V., 2010. Sea level changes during the last and present interglacials in Sal Island (Cape Verde archipelago). Global and Planetary Change 72, 302-317, doi: 10.1016/j.gloplacha.2010.01.006.